Published in final edited form as:

FASEB J. 2021 June ; 35(6): e21653. doi:10.1096/fj.202001921RR.

The function of the calcium channel Orai1 in osteoclast development

Lisa J. Robinson[1,2], **Jonathan Soboloff**[3], **Irina L. Tourkova**[4,5,6], **Quitterie C. Larrouture**[4,5,6], **Michelle R. Witt**[1,2], **Scott Gross**[3], **Robert Hooper**[3], **Elsie Samakai**[3], **Paul F. Worley**[7], **John B. Barnett**[2], **Harry C. Blair**[4,5,6]

[1]Department of Pathology, Anatomy and Laboratory Medicine, West Virginia University School of Medicine, Morgantown, WV, USA

[2]Department of Microbiology, Immunology & Cell Biology, West Virginia University Cancer Institute, West Virginia University School of Medicine, Morgantown, WV, USA

[3]Fels Cancer Institute for Personalized Medicine, Department of Medical Genetics & Molecular Biochemistry, Lewis Katz School of Medicine at Temple University, Philadelphia, PA, USA

[4]Department of Pathology, University of Pittsburgh, Pittsburgh, PA, USA

[5]Department of Cell Biology, University of Pittsburgh, Pittsburgh, PA, USA

[6]Pittsburgh VA Medical Center, Pittsburgh, PA, USA

[7]Solomon H. Snyder Department of Neuroscience, Johns Hopkins University School of Medicine, Baltimore, MD, USA

Abstract

To determine the intrinsic role of Orai1 in osteoclast development, Orai1-floxed mice were bred with LysMcre mice to delete Orai1 from the myeloid lineage. PCR, in situ labelling and Western analysis showed Orai1 deletion in myeloid-lineage cells, including osteoclasts, as expected. Surprisingly, bone resorption was maintained in vivo, despite loss of multinucleated osteoclasts; instead, a large number of mononuclear cells bearing tartrate resistant acid phosphatase were observed on cell surfaces. An in vitro resorption assay confirmed that RANKL-treated Orai1 null cells, also TRAP-positive but mononuclear, degraded matrix, albeit at a reduced rate compared to wild type osteoclasts. This shows that mononuclear osteoclasts can degrade bone, albeit less efficiently. Further unexpected findings included that Orai1$^{fl/fl}$-LysMcre vertebrae showed slightly reduced bone density in 16-week-old mice, despite Orai1 deletion only in myeloid cells; however,

Correspondence: John B. Barnett, Department of Microbiology, Immunology & Cell Biology, West Virginia University Cancer Institute, West Virginia University School of Medicine, Morgantown, WV 26506, USA. jbarnett@hsc.wvu.edu, Harry C. Blair, Pittsburgh VA Medical Center and the University of Pittsburgh, Pittsburgh, PA 15261, USA. hcblair@pitt.edu.

AUTHOR CONTRIBUTIONS

L. Robinson, J. Soboloff, and H. Blair designed research; L. Robinson, I. Tourkova, Q. Larrouture, M. Witt, S. Gross, R., and Hooper, E. Samakai performed research; P. Worley provided the founder Orai1$^{-/-}$ mice; L. Robinson, J. Soboloff, H. Blair, and J Barnett wrote the paper.

CONFLICT OF INTEREST

The authors declare that they have no conflict of interest.

SUPPORTING INFORMATION

Additional Supporting Information may be found online in the Supporting Information section.

this mild difference resolved with age. In summary, in vitro analysis showed a severe defect in osteoclast multinucleation in Orai1 negative mononuclear cells, consistent with prior studies using less targeted strategies, but with evidence of resorption in vivo and unexpected secondary effects on bone formation leaving bone mass largely unaffected.

Keywords

bone; mononuclear cells; Orai1 calcium channel; Orai1$^{fl/fl}$-LysMcre; osteoclast

1 | INTRODUCTION

The role of Orai1, a membrane calcium-selective ion channel, has been studied as a cause of immune dysfunction[1,2] with T-cell inactivation due to a calcium entry defect[3] Orai1 is activated by STIM1, a calcium sensor[4] and Orai1 is active in several types of cells where differentiation regulates cellular activity. STIM proteins are dynamic calcium signal transducers; Orai1 and STIM together reconstitute store-operated calcium channel function.[5,6]

We reported that global disruption of the Orai1 gene impaired the differentiation of osteoclasts and skeletal development. Interestingly, although global Orai1$^{-/-}$ mice lacked multinucleated osteoclasts, they did not develop osteopetrosis.[7] However, global Orai1$^{-/-}$ mice only survive for ~4 weeks due to non-skeletal effects, which complicates interpretation of the effects of Orai1. Mononuclear cells expressing osteoclast products occurred in global Orai1$^{-/-}$ mice, and we reported reduced, but significant mineral resorption by mononuclear osteoclast-like cells that formed in culture from peripheral blood monocytic cells when Orai1 is inhibited.[7] We attributed our unexpected finding of reduced osteoclast formation without increased bone density to decreased bone formation with retention of fetal cartilage. Micro-computed tomography and histology showed reduced cortical ossification, thinned trabeculae, and reduced alkaline phosphatase in global Orai1$^{-/-}$ animals compared with controls.

The limited lifespan and lack of cell specificity of conventional Orai1$^{-/-}$ knockout mice made it difficult to understand the in vivo role of Orai1 in osteoclast activity. Therefore, we examined the effect of Orai1 on osteoclasts using a conditional knockout mouse model. We obtained animals with an floxed Orai1, and bred these animals with mice expressing cre recombinase driven by the LysM promoter,[8] which is expressed in myeloid-lineage cells including osteoclast precursors, but few other cell types. We evaluated RANKL-induced differentiation in vitro using marrow from Orai1$^{fl/fl}$-LysMcre bone. As expected, Orai1-null osteoclasts exhibited loss of store-operated Ca^{2+} entry, and failed to form multi-nuclear cell in response to RANKL. Interestingly, although Orai1 deletion was restricted to myeloid cells, decreased bone density was observed in young mice only, which we attributed to secondary effects on bone formation. Overall, these findings reveal an intrinsic role for Orai1 in osteoclast differentiation limited to multinucleation. Our investigation further establishes that mononuclear “osteoclasts” have the capacity for bone degradation

and osteoclasts have an underappreciated role in the maintenance and differentiation of osteoblasts.

2 | METHODS

2.1 | Animals

Floxed Orai1 mice (Orai1$^{fl/fl}$) were made by Paul Worley's laboratory[9]; a construct with loxP flanking exons 2 and 3 of Orai1 was introduced via homologous recombination in embryonic stem cells. Orai1$^{fl/fl}$ mice were bred with B6.129P2-Lyz2tm1(cre) Ifo/J (JAX stock 004 781), briefly called LysMcre, at Jackson Labs (JAX, Sacramento, CA), as described,[10] making mice heterozygous for Orai1 and LysMcre. These were bred to produce the homozygous mice of interest, Orai1$^{fl/fl}$ LysM$^{wt/wt}$ and Orai1$^{fl/fl}$ LysM$^{cre/cre}$. Mice of both sexes were evaluated at age 16 weeks and 90 weeks. Animal work was approved by West Virginia University IACUC, protocol 1706006784.

2.2 | Genotyping

Mice were genotyped at JAX: the presence of the floxed gene was demonstrated by PCR, with flox-F ACC CAT GTG GAA AGA AA and flox-R TGC AGG CAC TAA AGA CGA TG primers producing a 505 bp amplicon.[9] For evaluation of cre recombination, the flox-F primer was paired with excision-R primer CAG AAA GAA CTA CAC AGA GAA ATC; excision results in a 520 bp amplicon. Mice with desired genotype from JAX were shipped for analysis. Genomic DNA was isolated from fresh lysates of whole marrow and spleen cells for PCR genotyping using REDExtract-N-Amp tissue PCR kit (Sigma, St. Louis, MO). To confirm Orai1 deletion from myeloid monocytic cells, spleens were gently dissociated in PBS pH 7.2, 0.5% BSA, and 2 mM EDTA. Cells were incubated with anti-F4/80-linked magnetic micro-beads and separated by AutoMACS (Miltenyi Biotech, Bergisch Gladbach, Germany). Aliquots of unsorted spleen cells were also frozen for Western blot analysis (see below). Genomic DNA for PCR was extracted from F4/80-positive and negative cells (Sigma REDExtract-N-Amp tissue PCR kit). Amplification used 94°C, 4 minutes, 30 cycles of 94°C, 30 seconds, 58°C, 30 seconds, and 72°C, 30 seconds and final extension 72°C, 2 minutes. Products were separated on 1.5% agarose.

2.3 | Tissue harvesting

Tissues were harvested from mice of each genotype at 16 or 90 weeks. Animals were weighed at sacrifice. For both age cohorts, spleen, and bones were collected. At 16 weeks, three limbs per animal were also used for bone marrow cell isolation and blood collected by cardiac puncture. The bones were fixed in 10% formalin for 48–72 hours, then transferred to 70% ethanol. Lumbar vertebrae 1–3 were used for histology and 4–6 were for micro computed tomography.

Analysis of blood cell types used the Hemavet 950-FS with mouse controls (Drew Scientific. Miami Lakes FL); results are mean ± SD.

2.4 | Cell culture and osteoclast differentiation

Marrow was flushed from long bones using a syringe. Red blood cells were osmotically lysed using 0.2% NaCl for 30 seconds followed by an equal volume of 1.4% NaCl. Cells were pelleted, resuspended in αMEM with 10% FBS, penicillin and streptomycin and 50 ng/mL mCSF (Shenandoah Biotech, Warwick PA), and plated at 5×10^6/mL, except for an aliquot frozen for gene expression studies (see below). After incubation overnight, non-adherent cells, including monocytic osteoclast precursors, were removed from adherent stromal cells and re-plated, with continued growth in m-CSF to favor survival of cells of monocytic lineage.[11,12] These cells were then used in experiments to evaluate calcium signaling, gene expression, and RANKL-induced differentiation.

To evaluate osteoclastogenesis, cells were plated at 40 000/well, on 24 well plates (Ibidi, Graefelfing, Germany) in αMEM with 10% FBS, penicillin and streptomycin and 50 ng/mL mCSF, then fed with or without 100 ng/mL RANKL (Shenandoah). After 5–7 days, tartrate resistant acid phosphatase (TRAP) activity was detected using diazotized fast garnet with the napthol AS-BI (Sigma TRAP staining kit). To evaluate mineral resorption,[13] cells were similarly cultured on osteoassay plates (Corning, Corning, NY). After treatment with or without RANKL for 5–7 days, media was aspirated and wells washed with 10% bleach for 5 minutes at room temperature, rinsed twice with distilled water and allowed to dry at room temperature for 3 to 5 hours. Images of individual pits or multiple pit clusters were acquired using a Lionheart imaging system (Biotek, VT). Images were stitched and resorption area was calculated with open source software Fiji (NIH). The combined area of resorption pits and trails was calculated manually.

Viable cell numbers in marrow cultures were quantified using Alamar Blue (Thermofisher, Pittsburgh, PA) according to the manufacturer's directions.

2.5 | Gene expression studies

Gene expression was evaluated by quantitative PCR in samples of whole bone marrow, spleen, or marrow monocytic cells cultured as described above for osteoclastogenesis. After cell lysis and RNA extraction using an RNeasy kit (Qiagen, Germantown, MD), mRNA was isolated by oligo-dT affinity (Qiagen). Synthesis of cDNA used random hexamers and Superscript III reverse transcriptase (Invitrogen). Quantitative PCR on a Stratagene MX3000P used SYBR green to monitor DNA synthesis. Reactions were run in duplicate, in 25 μL reaction volumes, with 12.5 μL of SYBR master mix, 250 nM primers and 1 μL of first strand cDNA. After 10 minutes at 95°C, amplification used 30 cycles of 30 seconds at 95°C, 30 seconds at 59°C, and 1 minute at 72°C. Products were analyzed by agarose gel electrophoresis and abundance relative to actin or GAPDH was calculated assuming linearity to log (initial copies).[14] Primers, except for genotyping (see text above) are listed in Table 1.

2.6 | Histomorphometry

Histomorphometry as described[15] used micro-computed tomography (μCT), at 6 μm resolution, on a Bruker Skyscan 1172 instrument with a 0.25 Al filter at 5 um 2 × 2 binning[16] and a bone density cutoff of 150 mg/cm^2. Examples of 8 μm thick vertebral sections are shown. Prior to analysis, bone samples were fixed overnight in 5% formalin

and kept at -20°C in 70% ethanol. For TRAP labeled bone surface, sections of bone were antibody labeled for TRAP and the area intersecting bone was measured as TRAP negative or TRAP labeled, as reported.[15,17] For cuboidal osteoblasts, decalcified sections labeled with hematoxylin and eosin were measured for bone surface and bone lined by cuboidal osteoblasts.

2.7 | Histology and Western blots

Western Blots used rabbit polyclonal anti-Orai1, from Alomone (Jerusalem, Israel), was used at 1:200. Labeled proteins were detected with peroxidase-linked anti-rabbit IgG and anti-mouse IgG (1:30 000) (Jackson Immuno-Research, West Grove, PA) by enhanced chemiluminescence. Mouse monoclonal anti-actin (clone AC-15), from Sigma (St Louis, MO), was used at 1:10 000 to re-probe for actin after membranes were stripped. *TRAP antibody:* sections were blocked in PBS and 2% milk, and incubated 18 hours with rabbit ACP5 anti-TRAP polyclonal antibody (Proteintech, Rosemont, IL) at 1:100, washed, and incubated with AlexaFluor488-labeled goat anti-rabbit IgG (Jackson ImmunoResearch, West Grove, PA) at 1:500. *Orai-1 antibody:* rabbit polyclonal-anti mouse Orai-1, laboratory produced by Ritchie et al,[18] was used for tissue labeling and Western Blots, as well as highly specific rabbit anti-Orai1 (extracellular) Antibody (ACC-062) from Alomone (Jerusalem, Israel). Antibodies showed Orai1 on Western blots (Figure 1C) with the Alomone Ab the most specific. Sections from 6 wild type (3 male, 3 female) and 6 conditional knockout animals were de-paraffinized at 67°C for 3 days, followed by xylene for 12 hours. Labeling was repeated in sections of three animals, and no antibody controls were done. Sections were blocked in PBS with 2% milk with 2 mM EDTA overnight at room temperature, followed by primary antibody at 1:100 in blocking solution (or no antibody controls) overnight. Secondary antibody anti-rabbit Cy3 (red) was added two hours at room temperature, followed by three rinses and fixation with 3.7% formalin. When indicated, counter staining used nuclear Hoechst (10 μg/mL). Imaging used a Nikon TE2000 microscope with a 14-bit 2048 × 2048-pixel monochrome charge-coupled device and RGB filters for color reconstruction (Spot, Sterling Heights, MI).

2.8 | Measurement of store operated calcium entry

Marrow cells isolated as described above, were plated on coverslips and maintained in 50 ng/mL m-CSF (Shenandoah). For calcium measurement[19] cells were loaded with 2 μM Fura-2 acetoxymethyl ester (Invitrogen) for 30 minutes at 25°C in 107 mM NaCl, 7.2 mM KCl, 1.2 mM $MgCl_2$, 11.5 mM glucose, 20 mM Hepes-NaOH, 1 mM $CaCl_2$, pH 7.2. Cells were washed and dye was allowed to de-esterify for 30 minutes at 25°C. Ca^{2+} measurements were made using a Leica DMI 6000B fluorescence microscope controlled by Slidebook Software (Intelligent Imaging, Denver, CO). Intracellular Ca^{2+} is shown as 340/380 nm ratios from single cells. Cells were stimulated with 10 μM uridine triphosphate (UTP) in absence of extracellular Ca^{2+} and after addition of 1 mM Ca^{2+}. Experiments were performed with or without the store-operated Ca^{2+} inhibitor N-methyl propanil 23818. Data used 15–20 cells per mouse in three or more experiments.

2.9 | Statistics

Statistical analysis used GraphPad Prism 7 Student's *t*-test unless otherwise specified. The magnitude of statistical difference was indicated as follows: $*P < .05$, $**P < .01$, and $***P < .001$. Data are mean ± SD unless noted.

3 | RESULTS

3.1 | Conditional knockout of Orai1 and genotyping

Generation of conditional Orai1-null mice is illustrated (Figure 1A). All animals produced were genotyped; verification of floxed status used primers from murine Orai1 flanking the 5' loxP insertion site. PCR performed on genomic DNA from lysates of whole bone marrow and spleen from Orai1$^{fl/fl}$-LysMcre mice reveal the floxed gene (Figure 1B-left). In addition, due to the subpopulation of myeloid cells, excision of the floxed segment of the Orai1 gene was also detected (Figure 1B-right). Western blots of spleen lysates (Figure 1C) show substantial loss of Orai1 expression at ~45 kD; since splenocytes contain both lymphoid and myeloid cells, this is consistent with expectations. Similarly, quantitative PCR (qPCR) for Orai1 in Orai1$^{fl/fl}$-LysMcre and Orai1$^{fl/fl}$-LysM-wt whole bone marrow shows substantial loss of Orai mRNA expression in the former (Figure 1D). To confirm that excision of the floxed segment of the Orai1 gene occurred selectively in the myeloid lineage, spleen cells were sorted based on expression of the murine monocyte-macrophage marker F4/80[20,21] by positive immunomagnetic selection. Using primers flanking the floxed segment of the Orai1 gene, a 520 bp product was amplified from genomic DNA of F4/80 positive myeloid cells confirming cre recombination; this was not detected for the F4/80 negative fraction that consists primarily of lymphocytes (Figure 1E). Quantitative PCR shows markedly decreased Orai1 in marrow cells from Orai1$^{fl/fl}$-LysMcre mice grown with mCSF, relative to cultured wild type cells (Figure 1F). Orai2 and Orai3 expression were also analyzed, and these showed no significant differences between wild type and conditional knockout (Figure S1).

3.2 | General features of Orai1$^{fl/fl}$ LysMcre animals

In contrast to mice with germline deletion of Orai1,[7] mice with conditional knockout of Orai1 in myeloid cells showed no reduction in size, based on femur length, or weight compared to controls (Table S1). No behavioral abnormalities were evident. Nor did any health abnormalities develop selectively in the conditional knockouts allowed to age to 90 weeks. We did observe that females of both genotypes showed significantly lower weights compared to males at 16 weeks (Table S2), though femur lengths were equivalent (not shown); by 90 weeks, both sexes of both genotypes showed wider variability in weights, with no significant differences found (not shown).

3.3 | Store-operated Ca^{2+} entry in osteoclasts

Store operated calcium entry was studies in cultures of the marrow monocytic cells from which osteoclasts arise. Cytosolic Ca^{2+} was monitored using Fura2AM by fluorescence microscopy. Wild type cells demonstrated typical store-operated Ca^{2+} entry kinetics when stimulated with UTP (Figure 2A). The haloanilide propanil inhibits SOCE via Orai1 in a concentration-dependent manner.[22] The analog N-methyl propanil (N-Me) exhibits

decreased toxicity but has similar efficacy as an Orai1 inhibitor; ~50% inhibition of store-operated Ca^{2+} entry by N-Me was observed in wild type osteoclasts (Figure 2B). An overlay shows the difference in SOCE with and without the N-Me inhibitor (Figure 2C). Identical experiments on marrow monocytic cells derived from Orai1$^{fl/fl}$-LysMcre mice showed no store-operated Ca^{2+} entry (Figure 2D). The addition of the Orai1-specific inhibitor N-Me showed no change in SOCE (Figure 2E); an overlay (Figure 2F) shows essentially identical Ca^{2+} entry with and without N-Me. These data show that store-operated Ca^{2+} entry via Orai1 was absent in osteoclast precursors from Orai1$^{fl/fl}$-LysMcre mice.

3.4 | Evaluation of osteoclast differentiation through expression of osteoclast markers

Expression of characteristic markers associated with bone cell differentiation[23] was determined by quantitative PCR (Figure 3). In wild type (WT) and Orai1$^{fl/fl}$-LysMcre (Orai1$^{-/-}$) whole marrow, mRNA for a bone differentiation inhibitor, produced primarily by osteoblasts, osteoprotegrin (encoded by the TNFRSF11B gene), was measured relative to GAPDH (Figure 3A). RANKL, an osteoclast differentiation protein,[24] the bone resorption proteins of osteoclasts cathepsin K, and ATPa3, as well as the key osteoclast marker TRAP, were also measured relative to GAPDH (Figure 3A). TRAP and RANKL were significantly reduced in the Orai1$^{-/-}$ whole marrow. Additional osteoblast products were assayed and RunX2, alkaline phosphatase (ALP), Type I collagen (Col1a1), and osteocalcin were also significantly reduced in the Orai1$^{-/-}$ whole marrow (Figure S2).

We evaluated expression of TRAP mRNA in wild type (WT) and Orai1$^{fl/fl}$-LysMcre (Orai1$^{-/-}$) marrow monocytic cells cultured without (Figure 3B, left) and with (Figure 3B, right) RANKL (Figure 3B). RANKL increased TRAP expression (Figure 3B), however, Orai1$^{-/-}$ cells produced significantly more TRAP than WT cells. This finding also mirrored the high TRAP expression visualized in vivo, see Figure 5C. Therefore, we evaluated other gene expression associated with osteoclast development and multinucleation in cells cultured with RANKL (Figure 3C). Expression of DC-STAMP, a protein previously shown to be required for osteoclast precursor fusion,[25] was decreased while NFATc1, a transcription factor that regulates osteoclast differentiation,[26] increased but not significantly. Similarly, the osteoclast-specific subunits of the V-ATPase, ATP6v0d2 and ATPa3[27–29] were also increased, although ATPa3 not significantly (Figure 3C). Monocytic cells cultured without RANKL showed no differences in assays for DC-STAMP, NFATc1, or the V-APase osteoclast subunit ATPa3 (Figure S3). A second subunit of the V-ATPase (ATP6v0d2) also did not show significant changes in the Orai1$^{fl/fl}$-LysMcre cells (not shown).

3.5 | In vitro production of multinucleated osteoclast-like cells from marrow of Orai1$^{fl/fl}$ LysMcre mice is greatly reduced

Bone marrow cells, harvested from wild type and Orai1$^{fl/fl}$-LysMcre animals, were grown in mCSF and then stimulated with RANKL to induce osteoclastic differentiation. Wild type multinucleated TRAP^{+} cells formed normally, both in culture (Figure 4A, left) and on layers of mineral-impregnated collagen (Figure 4B, left). RANKL and m-CSF-stimulated Orai1$^{fl/fl}$-LysMcre bone marrow cells expressed TRAP, but largely failed to form multinucleated syncytia (Figure 4A, right) or when cultured on mineralized matrix (Figure 4B, right). Quantification showed fewer TRAP^{+} Orai1$^{fl/fl}$-LysMcre cells (Figure

4C). Further, whereas RANKL stimulation led to a significant increase in $TRAP^+$ wild type cell size, $TRAP^+$ $Orai1^{fl/fl}$-LysMcre cells did not increase in size and were similar in size to unstimulated wild type bone marrow cells (Figure 4D). Further, the overall $TRAP^+$ cell area from wild type bone marrow cells stimulated with RANKL was 10 times higher than the $TRAP^+$ area in cultures from $TRAP^+$ $Orai1^{fl/fl}$-LysMcre bone marrow (Figure 4E). Nonetheless, cultures from $TRAP^+$ $Orai^{fl/fl}$-LysMcre bone marrow cells degraded matrix at ~40% of the rate of wild-type cells (Figure 4F), in keeping with the mild phenotype in vivo. Nuclei per cell were also counted in cultures as in Figure 4A (Figure 4G) with 5.5 nuclei per cell being the average in wild-type cells. In the $Orai^{fl/fl}$-LysMcre cells, the average was not statistically different from one nucleus per cell. In light of the reduced monocyte counts in the peripheral blood (Table 2), to exclude that reduced osteoclast differentiation in vitro reflected impaired survival or proliferation of precursors from $Orai1^{fl/fl}$-LysMcre bone marrow, cell survival/proliferation was evaluated for five days under non-differentiating conditions (Figure 4H). No changes were detected after plating of equal numbers of marrow cells from $Orai^{fl/fl}$-LysMcre and control animals.

3.6 | In vivo multinucleation and expression of TRAP in $Orai1^{fl/fl}$-LysMcre animals

Bone sections from 16-week-old WT and Orai1 floxed-LysMcre animals were labeled for expression of both TRAP and Orai1. Low power (500 μm) sections (Figure 5A) of bone were labeled for TRAP (top) and photographed in phase (bottom). Large TRAP-labeled cells were observed in the WT bone (marked in Figure 5A), but Orai1 floxed-LysMcre animals exhibited only mononuclear TRAP-labeled small cells. Sections from WT animals showed multinucleated Orai1-positive cells (Figure 5B, left), while sections from Orai1 floxed-LysMcre animals showed mononuclear Orai1-negative cells attached to bone (Figure 5B, middle) with a high power for clarity (Figure 5B, right). Additional sections show $TRAP^+$ multi-nucleated cells in samples from WT animals (Figure 5C, left), but only mononuclear cells in samples collected from Orai1 floxed-LysMcre animals (Figure 5C, middle), and a higher power for clarity (Figure 5C, middle and right). Interestingly, we observed that TRAP was primarily in the periphery of the mononuclear cells in Orai1 floxed-LysMcre animals (Figure 5C, right). In the absence of any true osteoclasts (multinucleated TRAP-positive cells) in the conditional knock-out, meaningful statistical analysis of osteoclast number (N.Oc/BS) was not possible. As an approximation of osteoclast surface (Oc.S) we assessed TRAP labeled surface area as a function of total bone surface; this revealed a significant reduction in the $Orai1^{fl/fl}$-LysMcre animals (Figure 5D). Further, osteoblast surface (Ob.S) was estimated from surface with cuboidal bone lining cells (Figure 5E); in the case of the $Orai1^{fl/fl}$-LysMcre animals, these are also Orai1 positive while the TRAP expressing mononuclear cells are, as shown above, negative for Orai1. The reduction in osteoblast surface was similar and significant ($P < .03$, n = 3). There was also a trend to a reduction in osteoblast numbers (N.Ob/BS) but this did not reach statistical significance (Figure S2/S4).

3.7 | Reduced bone formation in $Orai1^{fl/fl}$-LysMcre animals

In 16-week-old animals, wild type vertebrae had typical morphology (Figure 6A,B, left panels); while $Orai1^{fl/fl}$-LysMcre vertebrae had reduced trabecular bone (Figure 6A,B, right panels), visualized by μCT (A) or in H&E-stained decalcified sections (B). The distinct appearance of bone in $Orai1^{fl/fl}$-LysMcre animals corresponded with increased mean

trabecular separation, decreased intersection surface which reflects connectivity, as well as reduced bone volume, and reduced BV/TV in Orai1$^{fl/fl}$-LysMcre animals (Figure 6C) (all $P < .001$). Bone forming surface was estimated (Figure 5D, above); bone was not calcein labeled, reducing the parameters that could be determined by standard histomorphometry. Note that TRAP surface and estimated bone forming surface (Figure 5D,E) were similar in keeping with mild bone mass differences between wild type and Orai1$^{fl/fl}$-LysMcre vertebrae. No multinucleated TRAP positive cells were identified in multiple sections from Orai1$^{fl/fl}$-LysMcre mice, resulting osteoclast (Oc.N) of essentially zero in the conditional knockout, precluding further assessment (Figure S4). In older animals, differences were no longer significant: microCT of vertebrae from 90-week-old animals, in contrast to 16-week-old animals, showed equivalent bone density and histomorphometric parameters for wild type and Orai1$^{fl/fl}$-LysMcre animals (not illustrated).

3.8 | Orai1$^{fl/fl}$-LysMcre animals showed complex changes in blood cells other than mononuclear cells

Orai1$^{fl/fl}$-LysMcre animals had reduced blood cell counts, except for neutrophils. Peripheral blood cell phenotypes measured using the Hemavet system (Methods) showed 40%-60% reductions in total WBC, monocytes, lymphocytes, eosinophils, and basophils, but not in the neutrophils (Table 2).

4 | DISCUSSION

Orai1 expression affected both osteoblast and osteoclast differentiation in global Orai1 knockouts.[7,30] Further, Orai1 has a critical function in osteoclast differentiation, as studied in Raw264.7 mouse pre-osteoclast-like cells in vitro.[31] Nevertheless, many questions remain about the functions of Orai1 in bone[32]; these include difficulty separating the roles of Orai1 in osteoclasts versus osteoblasts to define its contribution to bone degradation and formation.

To address these questions, we used selective deletion of Orai1 in the myeloid lineage by breeding LysMcre and Orai1-floxed mice. This approach confirmed that Orai1 is essential for store-operated Ca^{2+} entry in Orai1-null myeloid-derived cells (Figure 2) and is required for osteoclast multinucleation both in vivo and *in vitro* (Figures 4 and 5). While the current investigation clearly implies that the requirement of Orai1 for osteoclast multinucleation is an intrinsic property of myeloid cells, the mechanism underlying the apparent Orai1-dependence of precursor fusion remains unclear. The reduced monocyte counts we observed in the peripheral blood raised the possibility that a lack of multinucleated osteoclasts might simply reflect a deficiency in the survival or proliferation of their precursors. However, no differences in marrow monocytic cell numbers were observed when Orai1$^{-/-}$ and WT marrow were cultured in vitro (Figure 4H). Further, defects in multinucleation were still observed when equal numbers of osteoclast precursors were used (Figure 4A,B).

The calcium-dependent transcription factor NFATc1 is a major driver of osteoclastogenic differentiation.[33] Since loss of Orai1-mediated calcium influx would be expected to lead to inadequate NFATc1 activation, this could have accounted for the failure of multinucleated osteoclast formation. To investigate this further, we examined osteoclast marker expression in culture, comparing precursors from Orai1$^{fl/fl}$-LysMcre to controls. Quantitative PCR

data confirmed reduced expression of osteogenic factors due to the absence of Orai1 (Figure 3A). Tartrate-resistant acid phosphatase mRNA was reduced in marrow cells from Orai1$^{fl/fl}$-LysMcre mice by ~20% ($P < .02$). Expression of RANKL, which drives osteoclast maturation and is produced by non-myeloid cells,[24] was reduced by half ($P < .02$). Other osteoclast proteins in whole marrow cells including Cathepsin K (Cath K) and the osteoclast hydrogen pump ATPa3 exhibited a trend to lower expression in Orai1$^{fl/fl}$-LysMcre animal marrow (Figure 3A), but were not statistically different. Molecules produced by osteoblasts, RunX2, osteocalcin, alkaline phosphatase and type I collagen in whole marrow cells were reduced ~40% on average (Figure S2). Differences in peripheral blood cell counts were seen, with in general fewer cells in the Orai1$^{fl/fl}$-LysMcre animals, but without a clear relation to bone parameters (Table 2).

Further analysis of mononuclear cells from wild type and Orai1$^{fl/fl}$-LysMcre animals with and without RANKL was performed (Figure 3B,C; Figure S3). NFATc1, a key regulator of osteoclast differentiation,[26,33] and V-ATPase subunits active in bone resorption, ATPa3[27] as well as ATP6v0d2[29,30] were assayed. However, no deficits in NFATc1 expression were detected and another protein linked to osteoclast function, ATP6v0d2, was actually increased in cultures of Orai1$^{fl/fl}$-LysMcre marrow cells (Figure 3C). Still more striking was the apparently enhanced induction of TRAP expression by RANKL in cells lacking Orai1 (Figure 3B). Other studies have shown a better correlation between Orai1 deficiency and decreased osteoclast marker gene expression,[30,31] but even in these studies reductions in osteoclast marker expression were often partial and sometimes absent.

The current investigation is the first to investigate myeloid-specific deletion of Orai1, the use of which reveals a specific role for Orai1-mediated Ca^{2+} signals in the expression of DC-STAMP and subsequent multinucleation and that expression of bone resorption components such as ATP6v0d2 and TRAP are independent of this pathway. DC-STAMP, shown to be critical for osteoclast multinucleation such that DC-STAMP germline knock-out results in osteopetrosis,[25,34] was indeed decreased in the Orai1-deficient marrow cell cultures. The result with DC-STAMP is particularly interesting, since knockout of this gene is believed to be another cause of failed osteoclast fusion without major effects on bone turn-over.[25] The results were in keeping with the essential role of NFATc1 as a precursor osteoclast development, the role of DC-STAMP as essential for multinucleation and the role of the V-ATPases in bone resorption, in this case, by mononuclear cells.

However, there were unexpected findings. The first is that bone turnover was not affected in a major way (Figure 6). Since these mice exhibited many TRAP-expressing mononuclear cells (Figures 5 and 6), the absence of increased bone mass in the conditional knockout suggests preserved bone degradation by this population. Bone degradation by mononuclear cells has long been hypothesized[35]; but has been difficult to prove. The current demonstration of matrix degradation in vitro and lack of osteopetrosis in vivo provides strong independent evidence for this concept. Note that Orai1-negative mononuclear cells effecting essentially normal bone degradation expressed normal quantities of ATPa3 and increased levels of ATP6v0d2, the bone specific subunits of the H^+ secreting H^+-ATPase[23,29] (Figure 3). Hence, despite work by other groups indicating a wider role for Orai1 in

osteoclast differentiation and function,[31] our investigations support a role for Orai1, at least in large part, being limited to multinucleation.

The current investigation definitively demonstrates that the requirement of Orai1 for osteoclast multinucleation is an intrinsic property of myeloid cells. In our model, it appears that the expression of other bone resorption components such as ATPa3, ATP6v0d2 and TRAP are not dependent on this pathway. Our measured mRNA expression levels of DC-STAMP, which were decreased, and the increased ATP6v0d2 mRNA expression levels are inconsistent with the results reported by Hwang et al.[30] Further, our previous report did show some retained TRAP positivity after Orai1 siRNA knockdown.[7] Indeed, based on past investigations of conventional Orai1-KO mice, it was hypothesized that defects on osteoblast formation reflected a role for Orai1 in osteoblasts.[7,30] While that may be the case,[15] the current investigations reveal that loss of bone formation also occurs with the loss of multi-nuclear osteoclasts, presumably an effect of this population on osteoblast development or activity. While we have not established a detailed mechanism, production of RANKL by whole marrow in Orai1$^{fl/fl}$-LysMcre animals was decreased (Figure 3A). Hence, loss of multinucleated osteoclasts has indirect effects on osteoblasts. Future investigations may shed further insight into this intriguing finding.

In summary, this work reveals an essential role of Orai1 in bone differentiation, even when effects are specific to osteoclasts and pre-osteoclastic cells. This work further suggests that the formation of mature multinucleated osteoclasts requires store-operated calcium entry (Figures 2 and 5), although bone resorption does not require multinucleation. There are many studies indicating importance for calcium signals in bone formation, eg,[36–38] but previously not showing documented specificity for osteoclast or myeloid cell expression of Orai1 (also known as calcium-release activated calcium channels). Our findings reflect cell-lineage specific changes, unlike the general Orai1 knockout,[7,30] where bone degrading, bone forming, and other cell types also potentially involved in bone regulation, are affected. Ultimately, this investigation sheds new insight not only into the role of Orai1 in osteoclast differentiation, but also provides new insight into the functional significance of osteoclast multinucleation and the interplay between osteoclasts and osteoblasts during differentiation.

Supplementary Material

Refer to Web version on PubMed Central for supplementary material.

ACKNOWLEDGEMENTS

Supported in part by The Department of Veterans Affairs grant BX002490 and by The National Institutes of Health (USA) grants AR065407, AR076146, and U54GM104942.

Funding information

U.S. Department of Veterans Affairs (VA), Grant/Award Number: BX002490; HHS | National Institutes of Health (NIH), Grant/Award Number: AR065407; HHS | NIH | National Institute of Arthritis and Musculoskeletal and Skin Diseases (NIAMS), Grant/Award Number: AR076146; HHS | NIH | National Institute of General Medical Sciences (NIGMS), Grant/Award Number: GM104942

Abbreviations:

ALP	alkaline phosphatase
ATP6v0d2	alternate osteoclast V-ATPase
ATPa3	osteoclast V ATPase
CTSK	cathepsin-K
DC-STAMP	dendritic cell-specific transmembrane protein
GAPDH	glyceraldehyde-3-phosphate dehydrogenase
LysM	lysozyme
mCT	micro-computed tomography
N-Me	N-methyl propanil
Orai1	ORAI calcium release-activated calcium modulator 1
Osx	Osterix
qPCR	quantitative polymerase chain reaction
RANKL	receptor activator of nuclear factor kappa-B ligand
siRNA	small interfering RNA
STIM1	stromal Interaction Molecule 1
TRAP	tartrate-resistant acid phosphatase
UTP	uridine triphosphate

REFERENCES

1. Feske S, Gwack Y, Prakriya M, et al.A mutation in Orai1 causes immune deficiency by abrogating CRAC channel function. Nature. 2006;441:179–185. [PubMed: 16582901]
2. Gwack Y, Srikanth S, Oh-Hora M, et al.Hair loss and defective T-and B-cell function in mice lacking ORAI1. Mol Cell Biol. 2008;28:5209–5222. [PubMed: 18591248]
3. Feske S. ORAI1 and STIM1 deficiency in human and mice: roles of store-operated Ca2+ entry in the immune system and beyond. Immunol Rev. 2009;231:189–209. [PubMed: 19754898]
4. Wang Y, Deng X, Zhou Y, et al.STIM protein coupling in the activation of Orai channels. Proc Natl Acad Sci U S A. 2009;106:7391–7396. [PubMed: 19376967]
5. Soboloff J, Spassova MA, Tang XD, Hewavitharana T, Xu W, Gill DL. Orai1 and STIM reconstitute store-operated calcium channel function. J Biol Chem. 2006;281:20661–20665. [PubMed: 16766533]
6. Soboloff J, Rothberg BS, Madesh M, Gill DL. STIM proteins: dynamic calcium signal transducers. Nat Rev Mol Cell Biol. 2012;13:549–565. [PubMed: 22914293]
7. Robinson LJ, Mancarella S, Songsawad D, et al.Gene disruption of the calcium channel Orai1 results in inhibition of osteoclast and osteoblast differentiation and impairs skeletal development. Lab Invest. 2012;92:1071–1083. [PubMed: 22546867]

8. Clausen BE, Burkhardt C, Reith W, Renkawitz R, Forster I. Conditional gene targeting in macrophages and granulocytes using LysMcre mice. Transgenic Res. 1999;8:265–277. [PubMed: 10621974]

9. Ahuja M, Schwartz DM, Tandon M, et al.Orai1-mediated antimicrobial secretion from pancreatic acini shapes the gut microbiome and regulates gut innate immunity. Cell Metab. 2017;25:635–646. [PubMed: 28273482]

10. Rauch A, Seitz S, Baschant U, et al.Glucocorticoids suppress bone formation by attenuating osteoblast differentiation via the monomeric glucocorticoid receptor. Cell Metab. 2010;11:517–531. [PubMed: 20519123]

11. Swamydas M, Lionakis MS. Isolation, purification and labeling of mouse bone marrow neutrophils for functional studies and adoptive transfer experiments. J Vis Exp. 772013;e50586. 10.3791/50586

12. Tourkova IL, Dobrowolski SF, Secunda C, et al.The high-density lipoprotein receptor Scarb1 is required for normal bone differentiation in vivo and in vitro. Lab Invest. 2019;99:1850–1860. [PubMed: 31467425]

13. Boraschi-Diaz I, Komarova SV. The protocol for the isolation and cryopreservation of osteoclast precursors from mouse bone marrow and spleen. Cytotechnology. 2016;68:105–114. [PubMed: 25245056]

14. Bustin SA. Absolute quantification of mRNA using real-time reverse transcription polymerase chain reaction assays. J Mol Endocrinol. 2000;25:169–193. [PubMed: 11013345]

15. Blair HC, Kalyvioti E, Papachristou NI, et al.Apolipoprotein A-1 regulates osteoblast and lipoblast precursor cells in mice. Lab Invest. 2016;96(7):763–772. [PubMed: 27088511]

16. Bouxsein ML, Boyd SK, Christiansen BA, Guldberg RE, Jepsen KJ, Müller R. Guidelines for assessment of bone microstructure in rodents using micro-computed tomography. J Bone Miner Res. 2010;25:1468–1486. [PubMed: 20533309]

17. Parfitt AM, Drezner MK, Glorieux FH, et al.Bone histomorphometry: standardization of nomenclature, symbols, and units. Report of the ASBMR Histomorphometry Nomenclature Committee. J Bone Miner Res. 1987;2:595–610. [PubMed: 3455637]

18. Ritchie MF, Yue C, Zhou Y, Houghton PJ, Soboloff J. Wilms tumor suppressor 1 (WT1) and early growth response 1 (EGR1) are regulators of STIM1 expression. J Biol Chem. 2010;285:10591–10596. [PubMed: 20123987]

19. Mookerjee-Basu J, Hooper R, Gross S, et al.Suppression of Ca(2+) signals by EGR4 controls Th1 differentiation and anti-cancer immunity in vivo. EMBO Rep. 2020;21:e48904. [PubMed: 32212315]

20. Austyn JM, Gordon S. F4/80, a monoclonal antibody directed specifically against the mouse macrophage. Eur J Immunol. 1981;11:805–815. [PubMed: 7308288]

21. Waddell LA, Lefevre L, Bush SJ, et al.ADGRE1 (EMR1, F4/80) is a rapidly-evolving gene expressed in mammalian monocyte-macrophages. Front Immunol. 2018;9:2246. [PubMed: 30327653]

22. Zhou Y, Lewis TL, Robinson LJ, et al.The role of calcium release activated calcium channels in osteoclast differentiation. J Cell Physiol. 2011;226:1082–1089. [PubMed: 20839232]

23. Blair HC, Athanasou NA. Recent advances in osteoclast biology and pathological bone resorption. Histol Histopathol. 2004;19:189–199. [PubMed: 14702187]

24. Lo Iacono N, Blair HC, Poliani PL, et al.Osteopetrosis rescue upon RANKL administration to Rankl(−/−) mice: a new therapy for human RANKL-dependent ARO. J Bone Miner Res. 2012;27:2501–2510. [PubMed: 22836362]

25. Yagi M, Miyamoto T, Sawatani Y, et al.DC-STAMP is essential for cell-cell fusion in osteoclasts and foreign body giant cells. J Exp Med. 2005;202:345–351. [PubMed: 16061724]

26. Negishi-Koga T, Takayanagi H. Ca2+-NFATc1 signaling is an essential axis of osteoclast differentiation. Immunol Rev. 2009;231:241–256. [PubMed: 19754901]

27. Blair HC, Teitelbaum SL, Ghiselli R, Gluck S. Osteoclastic bone resorption by a polarized vacuolar proton pump. Science. 1989;245:855–857. [PubMed: 2528207]

28. Wu H, Xu G, Li YP. Atp6v0d2 is an essential component of the osteoclast-specific proton pump that mediates extracellular acidification in bone resorption. J Bone Miner Res. 2009;24:871–885. [PubMed: 19113919]

29. Kim HJ, Lee Y. Endogenous collagenases regulate osteoclast fusion. Biomolecules2020;10:705–717.

30. Hwang SY, Foley J, Numaga-Tomita T, Petranka JG, Bird GS, Putney JW Jr. Deletion of Orai1 alters expression of multiple genes during osteoclast and osteoblast maturation. Cell Calcium. 2012;52:488–500. [PubMed: 23122304]

31. Hwang SY, Putney JW. Orai1-mediated calcium entry plays a critical role in osteoclast differentiation and function by regulating activation of the transcription factor NFATc1. FASEB J. 2012;26:1484–1492. [PubMed: 22198385]

32. Robinson LJ, Blair HC, Barnett JB, Soboloff J. The roles of Orai and Stim in bone health and disease. Cell Calcium. 2019;81:51–58. [PubMed: 31201955]

33. Kar P, Nelson C, Parekh AB. Selective activation of the transcription factor NFAT1 by calcium microdomains near Ca2+ release-activated Ca2+ (CRAC) channels. J Biol Chem. 2011;286:14795–14803. [PubMed: 21325277]

34. Witwicka H, Hwang SY, Reyes-Gutierrez P, et al.Studies of OC-STAMP in osteoclast fusion: a new knockout mouse model, rescue of cell fusion, and transmembrane topology. PLoS ONE. 2015;10:e0128275. [PubMed: 26042409]

35. Kahn AJ, Stewart CC, Teitelbaum SL. Contact-mediated bone resorption by human monocytes in vitro. Science. 1978;199:988–990. [PubMed: 622581]

36. Cheng Z, Li A, Tu CL, et al.Calcium-sensing receptors in chondrocytes and osteoblasts are required for callus maturation and fracture healing in mice. J Bone Miner Res. 2020;35(1):143–154. [PubMed: 31498905]

37. Doroudi M, Schwartz Z, Boyan BD. Membrane-mediated actions of 1,25-dihydroxy vitamin D3: a review of the roles of phospholipase A2 activating protein and Ca(2+)/calmodulin-dependent protein kinase II. J Steroid Biochem Mol Biol. 2015;147:81–84. [PubMed: 25448737]

38. Xi G, D'Costa S, Wai C, Xia SK, Cox ZC, Clemmons DR. IGFBP-2 stimulates calcium/calmodulin-dependent protein kinase kinase 2 activation leading to AMP-activated protein kinase induction which is required for osteoblast differentiation. J Cell Physiol. 2019;234:23232–23242. [PubMed: 31155724]

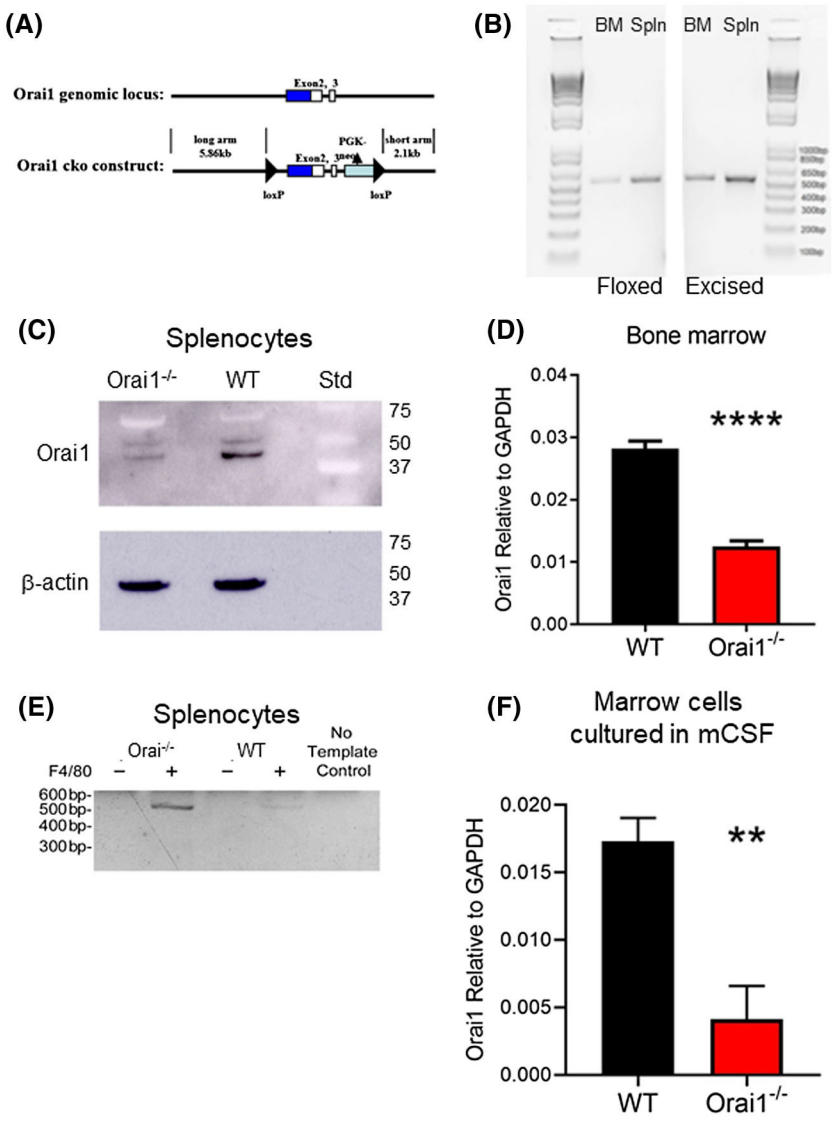

FIGURE 1.

Generation of Orai1$^{fl/fl}$-LysMcre mice and expression of Orai1 in bone marrow and splenocytes. A, Generation of Orai1$^{fl/fl}$-LysMcre mice (details in Methods). B, Genotyping of bone marrow and spleen of Orai1$^{fl/fl}$-LysMcre mice. PCR was performed on genomic DNA isolated from Orai1$^{fl/fl}$-LysMcre bone marrow and spleen, each including both myeloid and non-myeloid cell types. PCR using flox-F and flox-R primers (left panel), flanking the 5' loxP insertion site, produced 520 bp amplification products from marrow and spleen (lanes 2 and 3). Lane 1 shows 1 Kb plus DNA ladder. The result confirms the presence of floxed Orai1 in these animals; a 720 bp product would be amplified from a wild-type animal. PCR using flox-F and excision-R primers (right panel), upstream from the 5' LoxP site and downstream from the 3' LoxP site respectively, produced a 505 bp product from marrow and spleen (lanes 1 and 2, with 1 Kb plus DNA ladder in lane 3), confirming the presence of cells with cre-excision of Orai1; in the absence of excision, the primer sites are separated by over 2000 bp, so no product is amplified. C, Expression of Orai1 protein in

splenocytes by Western blot. The higher MW band in the WT and the Ora1i$^{-/-}$ cells is an artifact. D, Expression of Orai1 mRNA by qPCR using whole pooled bone marrow cells. N = 4, $P < .0001$. E, PCR showing Orai1 excision in monocytic vs. non-monocytic splenocytes separated by anti-F4/80 micro-beads. Products separated on 1.5% agarose are shown. F, Expression of Orai1 mRNA by qPCR in cultures of bone marrow cells from control (WT) and Orai1$^{fl/fl}$-LysMcre (Orai1$^{-/-}$), depleted of stromal cells, and grown with mCSF. N = 4, $P < .01$

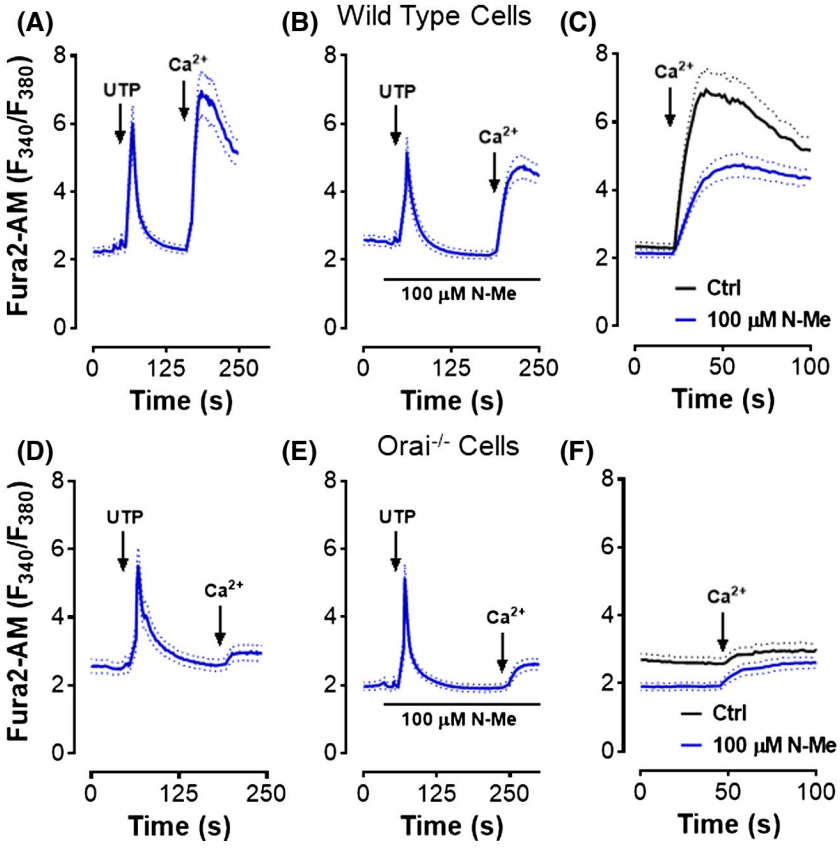

FIGURE 2.

Orai1$^{-/-}$ mononuclear cells show a severe defect in store-operated Ca^{2+} entry. Cells were plated on coverslips and loaded with Fura2-AM; cytosolic Ca^{2+} was monitored by fluorescence microscopy. Data average 15 to 20 cells per mouse, in three or more experiments. A-C, Mononuclear cells including osteoclast precursors from WT animals incubated one week in m-CSF. D-F, Orai1$^{-/-}$ cells after incubation one week in m-CSF. A,D, Cells stimulated with uridine triphosphate (UTP) (10 µM) in the absence of extracellular Ca^{2+}; 1 mM Ca^{2+} was added at the arrow. B,E, N-methyl-2-pyrrolidone (N-Me) (100 ∝M) was added prior to the addition of UTP. C, The Ca^{2+} entry portions of panels A and B are overlaid for comparison. F, The Ca^{2+} entry portions of panels D and E are overlaid for comparison

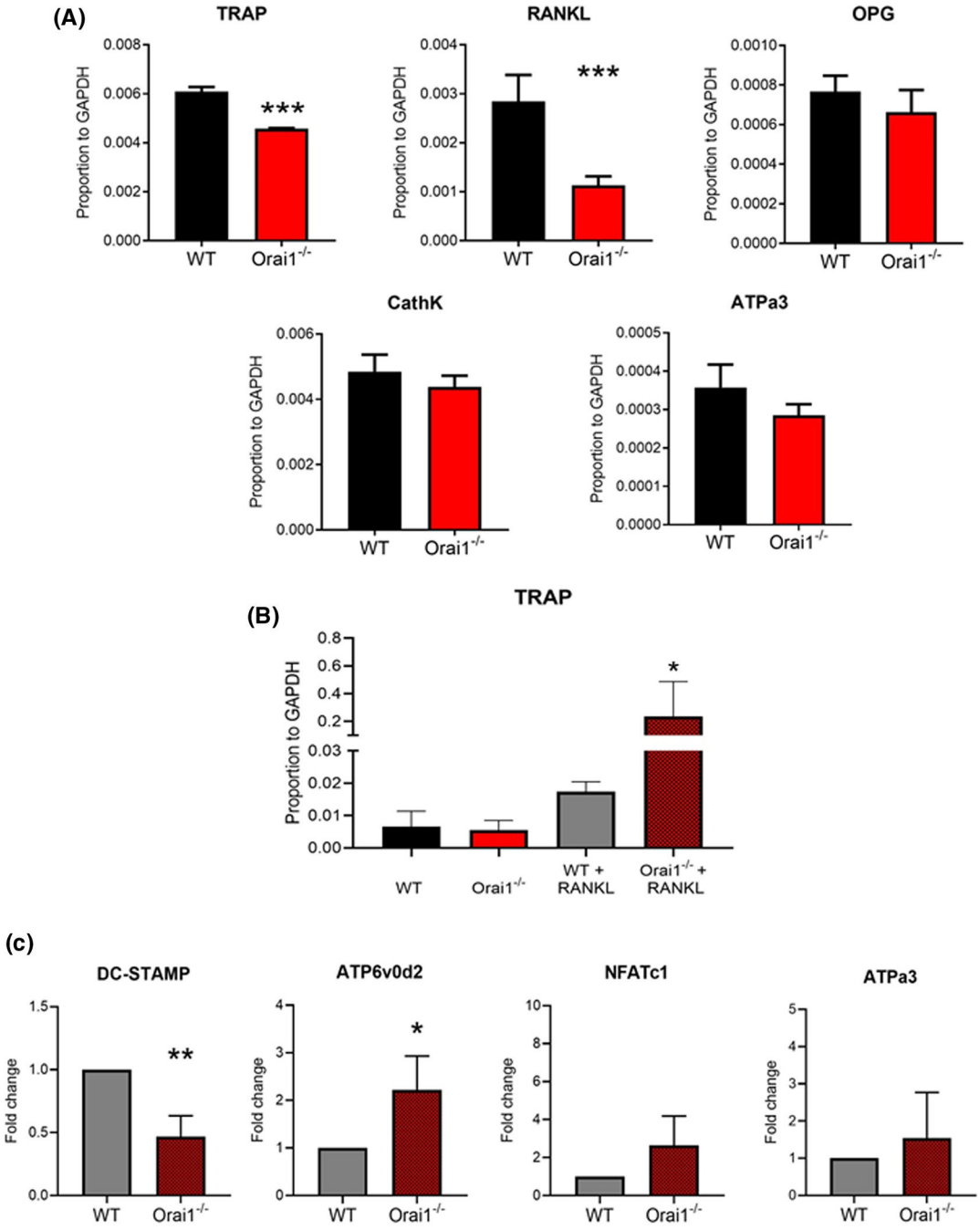

FIGURE 3.

Expression of osteoclast-related proteins in wild type and Orai1$^{fl/fl}$-LysMcre bone marrow and in macrophages with and without RANKL differentiation. A, In RNA from unstimulated whole marrow wild type (WT) and Orai1$^{fl/fl}$-LysMcre (Orai1$^{-/-}$) cells, expression of mRNA for a bone protein, osteoprotegerin (OPG), a bone produced osteoclast differentiation protein (RANKL) and bone resorption-related proteins of osteoclasts, cathepsin K, TRAP, and ATPa3, relative to GAPDH. In whole marrow, differences were statistically significant for TRAP and RANKL at $P < .02$. N = 4, mean ± SD. B, Expression of TRAP relative to

GAPDH determined by qPCR analysis of mRNA from control (WT) and Orai1$^{fl/fl}$-LysMcre (Orai1$^{-/-}$) bone marrow cells, depleted of stromal cells, and cultured with mCSF without (left) or with RANKL (right) for 7 days (N = 3, mean ± SD). Because data showed a non-normal distribution, results were analyzed by non-parametric ANOVA (Kruskal-Wallis test) with Dunn's test for multiple comparisons; TRAP expression was significantly greater ($P <$ .01, N = 3) in the RANKL-treated cells from Orai1$^{fl/fl}$-LysMcre animals compared to cells from controls with and without RANKL. C, Expression of osteoclast markers in RANKL-treated cultured marrow cells from Orai1$^{fl/fl}$-LysMcre (Orai1$^{-/-}$) animals determined by qPCR; results expressed as fold change compared to controls (WT); mean ± SD, N = 3. DC-STAMP is significantly reduced in the absence of Orai1 ($P <$ .001), while ATP6v0d2 shows a significant increase ($P <$ .01)

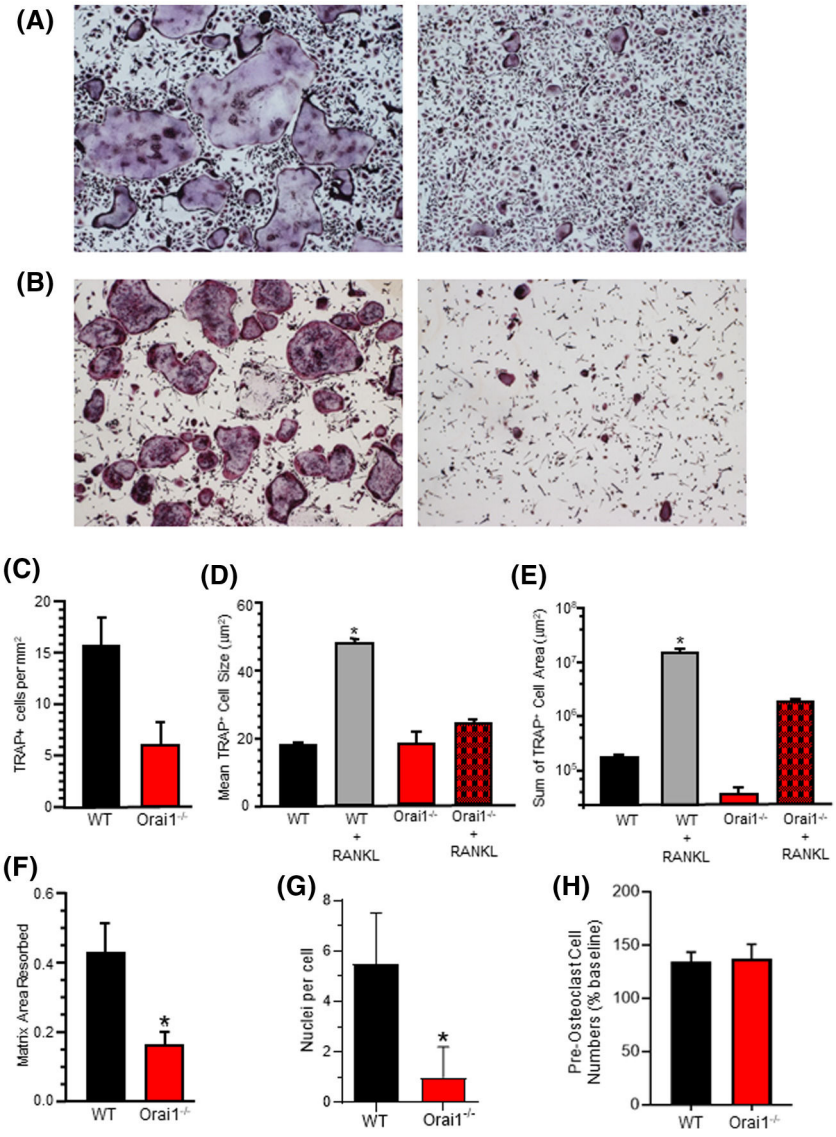

FIGURE 4.

In vitro osteoclastogenesis from bone marrow of Orai1$^{fl/fl}$-LysMcre and WT mice. A, Histomorphology of TRAP^{+} cells differentiated in vitro in RANKL plus m-CSF. Representative results from independent experiments using cells from three pairs of Orai1$^{fl/fl}$-LysMcre and WT mice. B, Histomorphology of TRAP^{+} cells differentiated in vitro in RANKL plus CSF-1 on mineralized matrix. Results are representative of independent experiments using cells from three pairs of Orai1$^{fl/fl}$-LysMcre and WT mice. C, TRAP^{+} cells per mm2 in cultures described in A above. D, Mean TRAP^{+} cell size in cultures described in A above. Wild type plus RANKL is significantly greater than all other groups. E, Mean TRAP^{+} cell area in cultures described in A above. Wild type plus RANKL is significantly greater than all other groups. F, Resorption of plate matrix coating by bone marrow TRAP^{+} cells from Orai$^{-/-}$ and WT mice differentiated in vivo. Data show the percent of matrix area resorbed, n = 4, mean ± SD $P < .001$. G, Nuclei per cell in cultures. Marrow cell cultures were stimulated with m-CSF and RANKL for one week and then

TRAP stained. The number of nuclei per TRAP+ cell was counted for Wild Type or Orai1$^{fl/fl}$-LysMcre mononuclear cells. The average number of nuclei per cell in wild-type cells was approximately 5.5 and in the Orai1$^{-/-}$ the average was approximately 1 per cell. These numbers are statistically different (n = 48, mean ± SEM, $P < .0001$). H, Evaluation of cell numbers in marrow cultures from control and Orai1 conditional knock-out mice. Cell numbers (per well of 96-well plate) evaluated by Alamar blue assay; shown are cell numbers after 24 hours as percentage of baseline ($t = 0$) cell numbers. Results (mean ± SD, N = 4) are representative of 3 independent experiments; no significant differences were detected

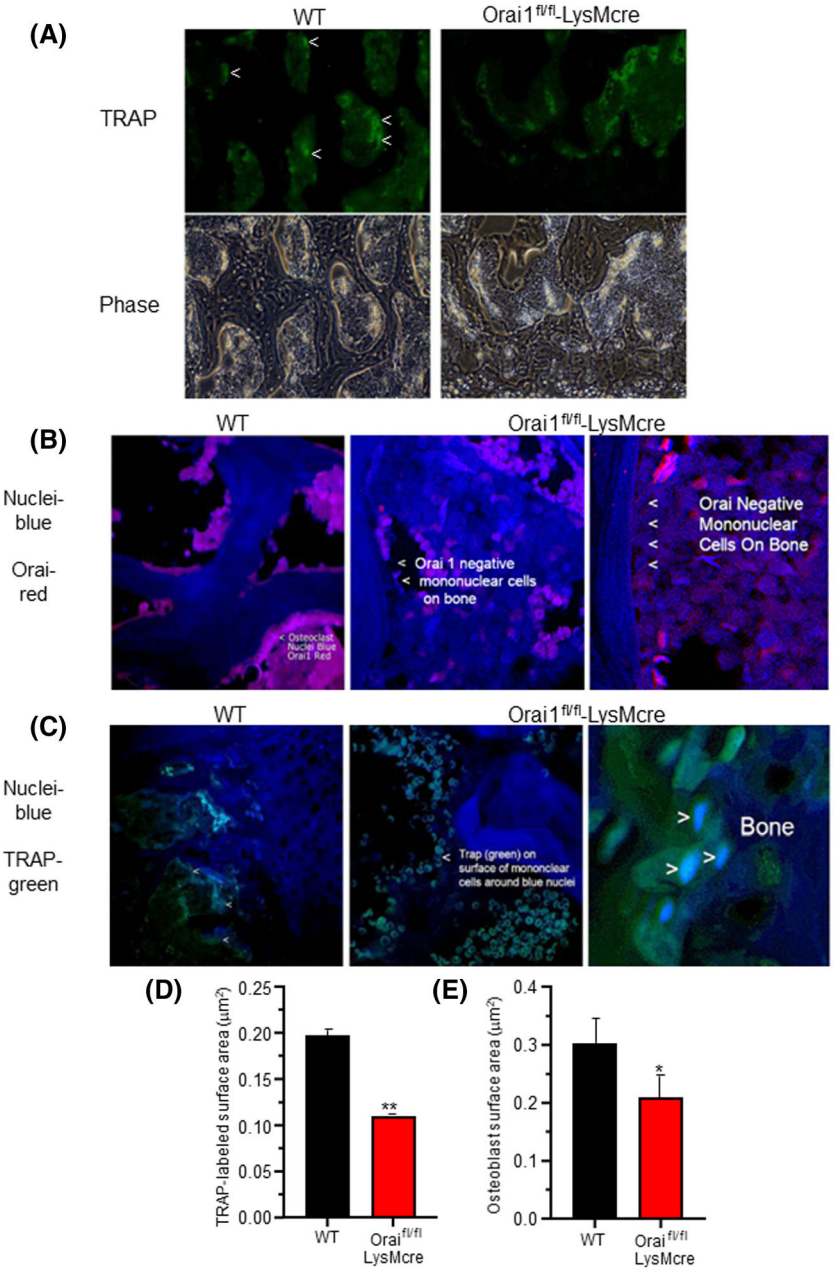

FIGURE 5.

Orai1$^{-/-}$ cells express osteoclast markers but do not multinucleate: Labeling of Orai1 and TRAP in WT and conditional Orai1$^{-/-}$ cells. In each case, WT is shown on the left and the LysM2 cre/Orai1-floxed bone on the right. A, Moderate magnification (500 µm across) sections of bone labeled for TRAP (top) and in phase (bottom) showing large cells (osteoclasts) in the WT (marked with <) and small cells (mononuclear cells) in the conditional knockout. Higher powers are shown below for clarity. B, Higher magnification (150 µm) sections labeled for Orai1 (red) and nuclei (blue) showing multinucleated Orai1 expressing cells in the wild type (left) and Orai1$^{-/-}$ mononuclear cells attached to bone in the conditional knockout (middle) with a high power (75 µm) section for clarity (far right).

C, TRAP (green) and nucleus (blue) labeled sections. A 200 μm field of the wild type (WT, left) shows multinucleated osteoclasts. A 100 μm field of the conditional knockout (Orai1$^{-/-}$, middle) shows TRAP labeled mononuclear cells. A higher power section of the conditional knockout (25 μm) is shown for clarity (far right). D, The TRAP labeled surface area (Oc.S/BS equivalent) as a function of total bone surface was measured. The TRAP labeled surface was decreased in the conditional knockout ($P < .01$, n = 3). E, Osteoblast surface area (bone formation surface) (Ob.S/BS) estimated as cuboidal bone lining cell area. The difference was similar to the difference in TRAP labeled surface ($P < .03$, n = 3)

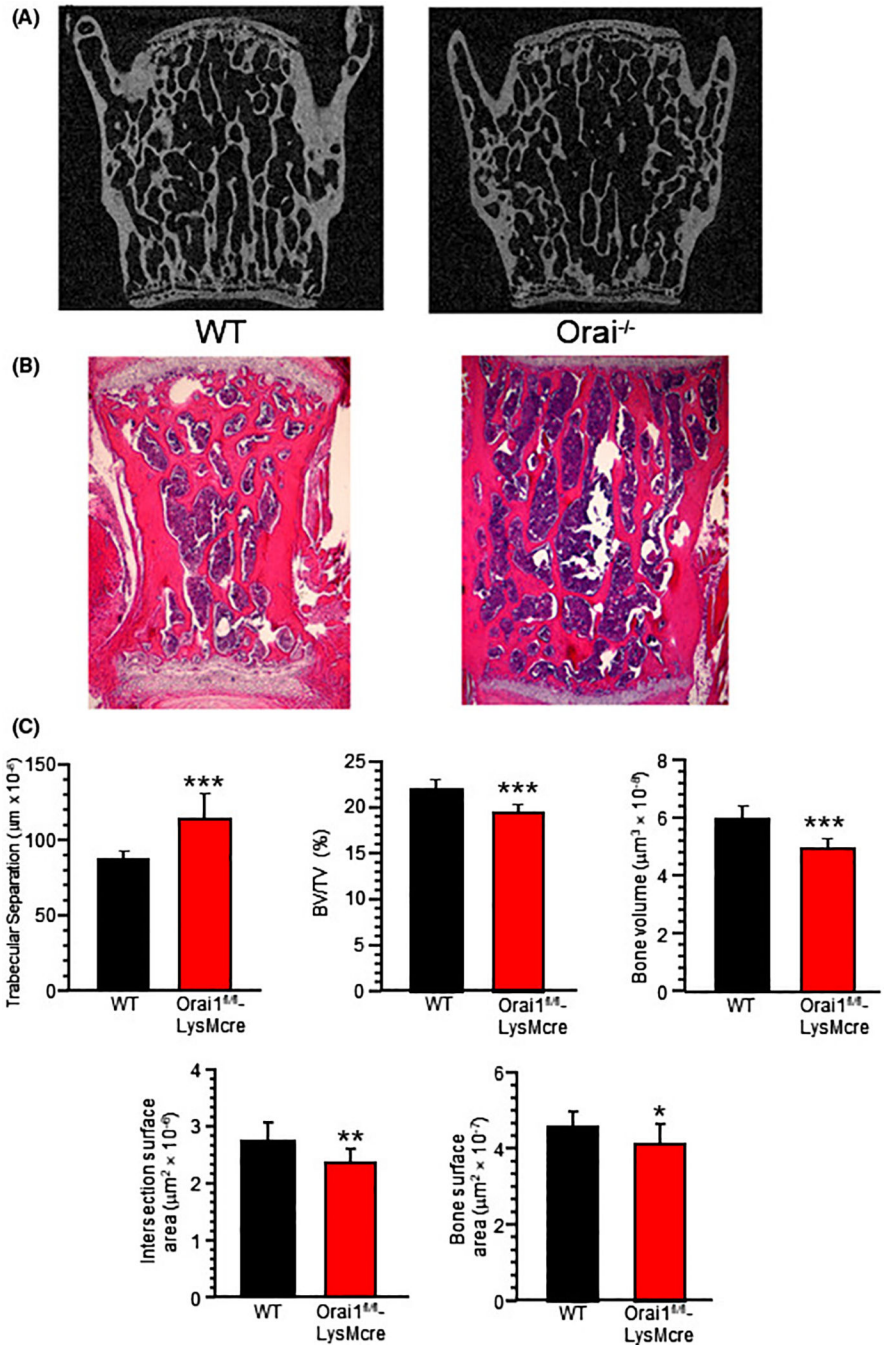

FIGURE 6.

Micro computed and hematoxylin and eosin-stained sections of wild type and LysMcre floxed Orai1 lumbar vertebrae at L4–5 show reduced bone in LysMcre floxed animals. A, Coronal projections of WT and Orai1$^{fl/fl}$-LysMcre vertebrae (L4). Sections are 2 mm wide. Analysis of micro-CT performed, at 6 µm resolution, on a Bruker Skyscan 1172 instrument. The central vertebral bone density in the Orai1$^{fl/fl}$-LysMcre is less than in the WT. Quantitative measurements below (C). B, Decalcified sections with hematoxylin and eosin staining. Sections are 2 mm wide. C, Static histomorphometry from the µCT

measurements., Measurements were different between wild type and the conditional KO with *P* values indicated in the figure, including Trabecular Separation (Tb.S), Bone volume/Total Volume (BV/TV), Bone Volume (BV), Intersection Surface (IS; area of intersection of trabeculae or connectivity) and Bone Surface (BS; total surface, site of all formation and resorption). N = 12. For TRAP surface area (OCS) and estimated bone formation surface (OBS), see Figure 5. (**P* < .05; ***P* < .01; ****P* < .001)

TABLE 1

PCR primers (mouse)

ALP NM_007431.2 Product size 131 bp (Alkaline phosphatase)

F—5′-ATCGGAACAACCTGACTGACCCTT-3′

R—5′-ACCCTCATGATGTCCGTGGTCAAT-3′

ATPa3 NM_178405.3 Osteoclast V ATPase Product size 163 bp

F—5′-TGACCACAAGCTGTCCTTGGATGA-3′

R—5′-AAGCTGACGACAGAACTTGACCCA-3′

ATP6v0d2 NM_175406 Alternate osteoclast V-ATPase probe Product size 192 bp

F—5′-GGAAGCTGTCAACATTGCAGA-3′

R—5′-TCACCGTGATCCTTGCAGAAT-3′

Cathepsin-K NM_007802.3 Product size 174 bp

F—5′-CAGCAGAGGTGTGTACTATG-3′

R—5′-GCGTTGTTCTTATTCCGAGC-3′

Col1a1 NM_007742.3 Product size 159 bp

F—5′-TTCTCCTGGCAAAGACGGACTCAA-3′

R—5′-AGGAAGCTGAAGTCATAACCGCCA-3′

DC-STAMP NM_029974 Product 139 bp

F—5′-CGGCGGCCAATCTAAGGTC-3′

R—5′-CCCACCATGCCCTTGAACA-3′

GAPDH NM_008084.3 Product size 184 bp (Glyceraldehyde-3-phosphate dehydrogenase)

F—5′-GTTGTCTCCTGCGACTTCA-3′

R—5′-GGTGGTCCAGGGTTTCTTA-3′

NFATc1 NM_01679.4 Product size 138 bp

F—5′-GGAACAGTTTAGACAGTACG-3′

R—5′-CCCTTTCACTGATGTCCTTG-3′

Osteocalcin NM_007541.2, NM_001037939.1 Product Size: 118 bp (Bone Gla Protein, BGLAP)

F—5′-ACCATCTTTCTGCTCACTCTGCTG-3′

R—5′-TATTGCCCTCCTGCTTGGACATGA-3′

Orai1 NM_175423.3 Product 192 bp

F—5′-TACTTAAGCCGCGCCAAGCT-3′

R—5′-GCAGGTGCTGATCATGAGGGC-3′

Orai2 NM_178751 Product 215 bp

F—5′-GGCCACAAGGGCATGGATTA-3″

R—5′-TGAGGGTACTGGTACTTGGTC

Orai3 NM_198424 Product 88 bp
F—5′-GCCTGCACCACTGTGTTAGTA-3′

R—5′-TGTTGCTCACGGCTTCAATATG

OPG NM_008764.3 Product 211 bp

F—5′-TTTGCCTGGGACCAAAGTGAATGC-3′

R—5′-AAGAAGCTGCTCTGTGGTGAGGTT-3′

RANKL NM_011613.3 Product size 83 bp

F—5′-GCTCCGAGCTGGTGAAGAAA-3′

Author Manuscript

Author Manuscript

Author Manuscript

R—5′-CCCCAAAGTACGTCGCATCT-3′

RunX2 NM_001145920.1 Product size 105 bp

F—5-ATGATGACACTGCCACCTCTGAC-3′

R—5-ACTGCCTGGGGTCTGAAAAAGG-3′

TRAP NM_001102405.1 Product size 174 bp

F—5′-CACGAGAGTCCTGCTTGTC-3′

R—5′-AGTTGGTGTGGGCATACTTC-3′

TABLE 2

Hematology values

Cell type[a]	Wild type[b]	Orai1$^{fl/fl}$-LysMcre[b]
WBC	4.788 ± 0.353	2.943 ± 0.307 ($P < .05$)*
Neutrophil	1.024 ± 0.115	0.929 ± 0.201
Lymphocytes	3.373 ± 0.241	1.875 ± 0.227 ($P < .05$)*
Monocytes	0.253 ± 0.038	0.121 ± 0.025 ($P < .05$)*
Eosinophils	0.143 ± 0.021	0.059 ± 0.011 ($P < .05$)*
Basophils	0.042 ± 0.007	0.017 ± 0.003 ($P < .05$)*
Platelets	1048 ± 211.3	805.1 ± 120.5
Mean platelet volume	5.971 ± 0.161	5.294 ± 0.176

[a] All values are $\times 10^3/\propto$l whole blood except Mean platelet volume (femtoliters).

[b] Mean ± SEM, n = 14 for wild type and n = 15 for Orai1$^{fl/fl}$-LysMcre.

* Significantly different by *t*-test.